Microporous and Mesoporous Materials 172 (2013) 206–212

Contents lists available at SciVerse ScienceDirect

Microporous and Mesoporous Materials

journal homepage: www.elsevier.com/locate/micromeso

Development of HZSM-5/AlMCM-41 hybrid micro–mesoporous material and application for pyrolysis of vacuum gasoil

Ana C.F. Coriolano [a,b,*], Cristiano G.C. Silva [a], Maria J.F. Costa [b], Sibele B.C. Pergher [b], Vinícius P.S. Caldeira [b], Antonio S. Araujo [b,*]

[a] UNP – Laureate International Universities, Av. Nascimento de Castro 1597, 59056-450 Natal, RN, Brazil
[b] Federal University of Rio Grande do Norte, Institute of Chemistry, 59078-970 Natal, RN, Brazil

ARTICLE INFO

Article history:
Received 31 May 2012
Received in revised form 15 January 2013
Accepted 19 January 2013
Available online 9 February 2013

Keywords:
Hybrid material
ZSM-5/MCM-41
Acidity
Vacuum gasoil
Pyrolysis

ABSTRACT

The pyrolysis of vacuum gasoil (VGO) was studied alone and in presence of HZSM-5/AlMCM-41 hybrid catalyst. This micro–mesoporous material was synthesized by the hydrothermal method using dual templates of tetrapropilamonium and cetyltrimethylammonium ions at different crystallization times. The obtained materials were washed and calcined for remotion of the organic templates. The characterization by X-ray diffraction, nitrogen surface area by the BET method, scanning and transmission electron microscopies, evidenced that typical MFI structure was embedded into the bulk of the MCM-41 matrix, in order to obtain the hybrid micro–mesoporous phase. The protonic form of the material was obtained by ion exchange with ammonium chloride solution and subsequent thermal treatment. The total acidity, as determined by *n*-butylamine adsorption, was equivalent to 0.75 mmol g^{-1}, in the temperature range of 300–500 °C, corresponding to strong acid sites. For catalytic reaction, a physical mixture of 10% of catalyst/VGO was decomposed in a thermobalance at heating rates of 5; 10 and 20 °C min^{-1}, from 100 to 550 °C. From TG/DTG data, applying the model-free kinetics, it was observed that the activation energy for the pyrolysis of VGO alone was *ca.* 125 kJ mol^{-1}. For VGO physically mixed to both AlMCM-41 and HZSM-5, the value decreased to *ca.* 80–90 kJ mol^{-1}, whereas for the hybrid, the value was the lowest, *ca.* 65 kJ mol^{-1}, evidencing the efficiency of the combined effect of the acid sites, crystalline phase and microporosity of ZSM-5 zeolite with the accessibility of the mesoporous of the AlMCM-41 ordered material. For determination of the catalytic properties, the samples of VGO and catalyst/VGO were submitted to pyrolysis-GC–MS system at 500 °C using helium as gas carrier. The VGO alone suffers decomposition to a wide range of hydrocarbons, typically C_{17}–C_{41}, while in the presence of catalyst, light fraction of hydrocarbons, in the range of liquefied petroleum gas (C_3–C_5), gasoline (C_6–C_{10}) and diesel (C_{11}–C_{16}) were obtained, evidencing that the HZSM-5/AlMCM-41 hybrid material is an effective catalyst for pyrolysis of VGO.

1. Introduction

Micro–mesoporous hybrid materials are defined as a combination of two inorganic structures deeply bonded through a homogeneous system, whose properties derivate from the individual characteristics of each one component associated with the synergistic effect of both. These materials are also known as micro–mesostructured solids, or hybrid zeolite-mesoporous materials. Recently, the synthesis of ordered mesoporous materials with MFI structured microporous walls has been reported [1]. These materials present well-ordered structures, activity and selectivity for application in the processing of voluminous molecules present in the heavy and ultra-heavy petroleum.

The Brazilian refineries are improving their processes in order to increase the production in light hydrocarbons, due to its high market value, as well as the optimization of the processing of low-value co-products, like atmospheric residues, vacuum gasoils and heavy oil wastes (sludges). The catalytic cracking of hydrocarbon over traditional Y and ZSM-5 zeolites is limited by the low accessibility to its micropores, which have diameters smaller than 1 nm. Moreover, mesoporous materials such as MCM-41 [1–3] and SBA-15 [4,5], which have pore diameter between 2 and 50 nm present physicochemical properties for adsorption and catalytic applications. To overcome these constraints, hybrid materials are very interesting, because they combine the high catalytic activity of zeolites with the easier accessibility of the mesoporosity. The

* Corresponding authors. Address: UNP – Laureate International Universities, Av. Nascimento de Castro 1597, 59056-450 Natal, RN, Brazil (A.C.F. Coriolano). Tel./fax: +55 84 3211 9240.
E-mail addresses: catarinaufrn@yahoo.com.br (A.C.F. Coriolano), araujo.ufrn@gmail.com (A.S. Araujo).

1387-1811/$ - see front matter © 2013 Elsevier Inc. All rights reserved.
http://dx.doi.org/10.1016/j.micromeso.2013.01.022

hybrid catalysts should be composed by crystalline/non-crystalline aluminosilicates phases with a combined micro–mesoporous structure, and are attracting attention of researchers due to their potential applications in catalysis and adsorption technologies for the chemical and petrochemical industries [6,7]. The silica MCM-41 is the main mesoporous material of the M41S family, created by researchers of Mobil Oil Research and Development Corporation [8,9]. The formation of the MCM-41 phase occurs according to the Liquid Crystal Template (LCT) mechanism, in which SiO_4 tetrahedron reacts with the surfactant template under hydrothermal conditions. The MCM-41 is formed by a hexagonal assembler of silicon tubes resulting in a pore structure, characterized by presenting high specific surface area, in one-dimensional regular pore system with pore diameter that systematically varies from 2 to 10 nm, possessing a high thermal stability and a moderate acidity.

In this work, we synthesized the micro–mesoporous structures of ZSM-5/MCM-41, using the route of dual template. In the synthesis, the properties of the MCM-41 were adjusted by the isomorphous substitution of Si by the trivalent cation Al^{3+}, resulting in the AlMCM-41 mesoporous material. The MCM-41 acts as a support for growth of the zeolitic nanocrystals type ZSM-5 embedded into the mesoporous bulk, resulting in the ZSM-5/MCM-41 hybrid material [10–12]. The morphologic properties, such as surface area of the composite is approximately half of the surface area of the conventional MCM-41, and the formation of walls with the double of the density, characterizes the ZSM-5/MCM-41 hybrid material, resulting in a high stability material for catalytic applications.

The obtained materials were evaluated for cracking or pyrolysis of Vacuum Gasoil (VGO) and compared with those of HZSM-5 and AlMCM-41 catalysts. These evaluations were carried out by thermogravimetry. This method has been widely applied for degradation of heavy oil [13] and pyrolysis of polyethylene [14–17]. The VGO corresponds to the residue stream obtained in the vacuum distillation of the residue generated at the atmospheric distillation of crude oil. The VGO is composed basically by *n*-paraffins with number of carbons distributed in range from C_{20} to C_{40} [18]. The catalytic activity and product distributions were accomplished by coupled pyrolysis gas chromatography and mass spectrometer (pyrolysis-GC/MS).

2. Experimental

2.1. Hydrothermal synthesis

The composite ZSM-5/MCM-41 hybrid materials was synthesized by the hydrothermal method, based on experimental procedure adapted from the synthesis of Huang et al. [10], and molar composition of $1SiO_2{:}0.32Na_2O{:}0.033Al_2O_3{:}0.20TPABr{:}0.16CTMABr{:}55H_2O$.

Aqueous solutions of tetrapropylammonium bromide (TPABr, Sigma–Aldrich, 99%), as a template of the zeolite structure, and sodium aluminate (Riedel-de Haën, 53%wt Al_2O_3 and 45%wt Na_2O) were combined with a solution of sodium silicate containing 7.4%wt Na_2O, 25.4%wt SiO_2 (Merck) and 67.2% of deionized H_2O. The reaction mixture was stirred at room temperature until obtaining a white gelatinous suspension. Afterwards, an aqueous solution of cetyltrimethylammonium bromide (CTMABr, Vetec, 98%) was added as a template to the mesoporous molecular sieve, and the final mixture was stirred for obtain a homogeneous gel. This reactive hydrogel was transferred to a Teflon-lined stainless steel autoclave, where the process of crystallization of the material was performed in two stages. The first stage of crystallization was performed at 100 °C at pH 11 for 2 days. The second stage of crystallization (or re-crystallization) was conducted at 125 °C and pH 9–10, between periods ranging from 6 to 12 days. The material was afterwards filtered, washed and calcined to obtain the sodium form ZSM-5/AlMCM-41. The as-prepared material was calcined at 540 °C for 1 h in N_2 atmosphere and then for 5 h in synthetic air at the same temperature using a dynamic flow of 100 mL min^{-1}. The temperature was increased from room temperature to 540 °C at a heating rate of 10 °C min^{-1}.

The HZSM-5/AlMCM-41 acid form was obtained by ion exchange with NH_4Cl solution and its subsequent thermal treatment. In order to obtain the optimized structures of the hybrid material, variations in the synthesis time were carried out. For comparison of the properties of the hybrid material, the acid form of the aluminum-containing MCM-4 was prepared using the method previously reported [19], with molar composition of $4SiO_2{:}1Na_2O{:}0.13Al_2O_3{:}1CTMABr{:}200H_2O$.

2.2. Characterization of the materials

For characterization of the materials, the XRD measurements were carried out, using CuKα radiation in 2θ angle range of 1–7° and 7–50°, low-angle and wide-angle, respectively, for calcined samples, with step of 0.02°, on a Shimadzu XRD 6000 X-ray equipment. The specific surface area (S_{BET}) was determined by N_2 adsorption–desorption, on a Quantachrome NOVA-2000 equipment, at 77 K, according to the Brunauer–Emmett–Teller (BET) method [20] in the relative pressure P/P_0 in the range of 0.05–0.95. The samples were previously outgassed by treatment at 200 °C for 3 h under vacuum. Pore size distributions (D_p) were calculated according to Barrett–Joyner–Halenda (BJH) algorithm [21] and the total pore volume (V_t) was determined according to the *t*-plot method. The peak of Bragg diffraction around 23° (2θ) was used to determine the relative crystallinity (C_{REL}) from the zeolite phase in the hybrid composite, taking as pattern the diffractogram of the sample of commercial ZSM-5. The SEM measurements were performed using a JEOL JSM-6360 instrument. The samples were ultrasonically dispersed in H_2O at a concentration of 1 mg mL^{-1}, and a drop of the suspension was deposited on a holey carbon copper grid, and then dried at 100 °C.

2.3. Determination of the acidity

In order to determine the density of the acid sites of the catalysts, *n*-butylamine adsorption experiments on the HZSM-5/AlMCM-41, HAlMCM-41 and HZSM-5 samples were performed in a reactor containing *ca.* 0.1 g of catalyst, which was activated initially at 400 °C, under N_2 flowing at a rate of 100 mL min^{-1}, for 2 h. After this activation, the temperature was reduced to 95 °C and the N_2 flow was passed through a saturator containing liquid *n*-butylamine. The *n*-butylamine saturated with N_2 stream was directed to the reactor containing the samples for 1 h. Afterwards, pure N_2 was passed once again over the samples for 40 min in order to remove the physically adsorbed *n*-butylamine. TG analyses were performed in a Mettler equipment, TGA/SDTA851 model, using N_2 as a gas carrier flowing at 25 mL min^{-1}. The samples were heated from room temperature up to 900 °C, at a heating rate of 10 °C min^{-1}. The procedure used for determination of the total acidity was previously reported [22–26].

2.4. Pyrolysis of vacuum gasoil (VGO)

The thermal and catalytic pyrolysis of VGO was performed by thermogravimetry. The catalyst/VGO mixture, at proportions of *ca.* 10% in mass of catalyst, were heated from room temperature up to 900 °C, at a heating rate of 5; 10 and 20 °C min^{-1}. The Vyazovkin model-free kinetics [27,28] was used to evaluate the kinetic parameters relative to thermal and catalytic degradation of VGO. The potential application of hybrid HZSM-5/AlMCM-41

material for the pyrolysis reaction of VGO was investigated and compared with those of pure HZSM-5 and AlMCM-41 catalysts. The activation energies relative to the thermal and catalytic pyrolysis of VGO were determined. Also, the process was carried out in a microreactor at 500 °C, under helium flowing at 25 mL min^{-1}. The pyrolizer was coupled to the gas chromatograph and mass spectrometer equipment, GC/MS QP 2010 Series from Shimadzu. The products were analyzed using a capillary column UA5-30M-0.25F (30 m × 0.25 mm i.d., 0.25 μm film thickness).

3. Results and discussion

3.1. Characterization from XRD and nitrogen adsorption

The analysis of low-angle and wide-angle X-ray of the calcined samples, are respectively, presented in Fig. 1(a) and (b). Comparative study of the XRD patterns of the standard AlMCM-41 and HZSM-5 samples with those of the hybrid materials were accomplished aiming to obtain an optimized structure.

The steps of crystallization were accomplished at 125 °C and pH 9–10, for a period of 6, 7, 8, 9 and 12 days, and the samples were signed as: ZSM-5/AlMCM-41(X), where "X" represents the quantity of days of crystallization. From XRD, it was observed a peak for 2θ between 1.5° and 2.5°, which is characteristic of the Bragg reflection plane (100), and this is a clear evidence of the presence of the MCM-41 structure. The Bragg planes (110), (200), and (210) were not clearly observed, that demonstrates a poor ordering of the mesoporous structure of the hybrid samples. The best preservation of long-range ordered hexagonal MCM-41 with low formation for the zeolite MFI-type (ZSM-5) was attributed to the recrystallization in a period of time of 7 days.

Fig. 2 illustrates the N_2 adsorption–desorption isotherms at 77 K and the pores size distribution curves, calculated by applying the BJH model, for the ZSM-5/AlMCM-41(7) hybrid material, which was optimized for 7 days of synthesis, and was compared with typical isotherm type IV for AlMCM-41 and type I for ZSM-5 zeolite.

Confirming the results of XRD, the hybrid ZSM-5/AlMCM-41(7) sample presented a N_2 adsorption isotherm type IV, typical of uniform mesoporous material according to the IUPAC nomenclature [29], ensuring the permanence of the mesoporous phase in parallel

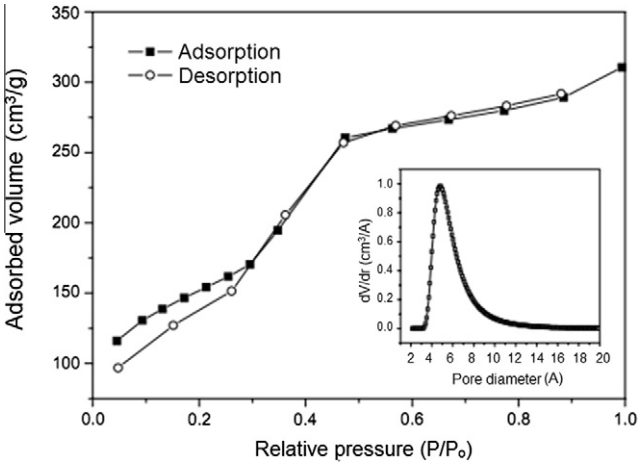

Fig. 2. N_2 adsorption (-■-) and desorption (-○-) isotherms at 77 K for the ZSM-5/AlMCM-41(7) hybrid material.

with the microporous phase, alongside a satisfactory distribution of pore size, with mesopores around 5 nm.

The textural and structural properties of the different catalysts obtained from the results of XRD and N_2 adsorption–desorption, were summarized in Table 1. The determination of specific surface area (S_{BET}), pore diameter (D_p) and total pore volume (V_t) were obtained, by BET, BJH and *t*-plot methods, respectively.

The mesoporous parameter of the MCM-41 and hybrid materials (a_0) represent the distance between the pore centers of the hexagonal structure, obtained from the interlayer plane (100) of the X-ray diffractogram, and was calculated applying Eqs. (1) and (2). It represents the sum of the medium diameter of its porous (D_p) plus the size of the silica wall thickness (W_t), as can be clearly viewed in Fig. 3, for the hexagonal array of the mesopores materials. Also, knowing the pore size diameter (D_p), obtained from nitrogen adsorption data, and the mesoporous parameter (a_0), from XRD, the wall thick (W_t) can be easily obtained, applying Eq. (3).

$$\frac{1}{d(hkl)^2} = \frac{4(h^2 + hk + l^2)}{3_{a_0^2}} + \frac{l^2}{c} \quad (1)$$

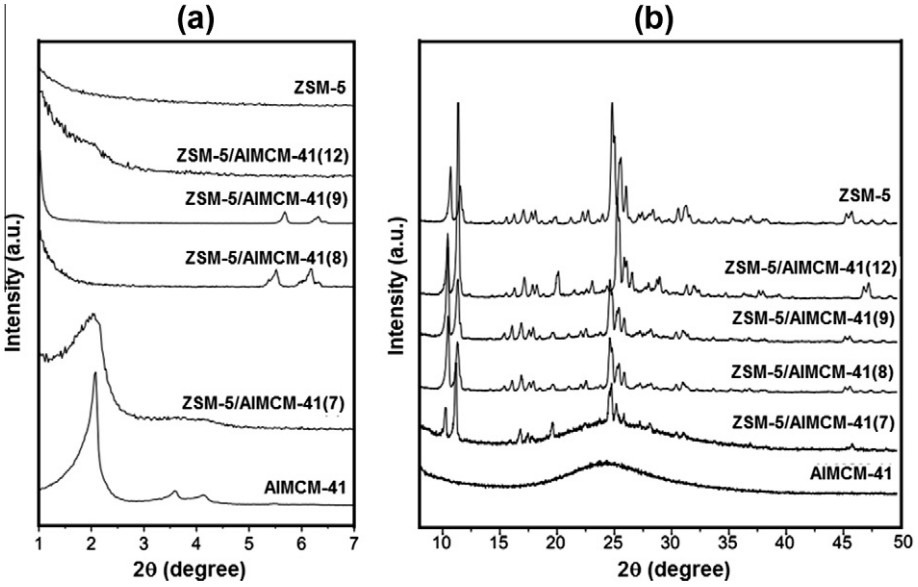

Fig. 1. (a) Low-angle and (b) wide-angles XRD spectra of the calcined samples.

Table 1
Textural properties of the MCM-41/ZSM-5(7), Al-MCM-41 and ZSM-5.

Sample	Mesopore phase		Micropore phase	Textural properties		
	a_0 (nm)	D_p (nm)	C_{REL} (%)	S_{BET} ($m^2\ g^{-1}$)	V_t ($cm^3\ g^{-1}$)	W_t (nm)
ZSM-5/AlMCM-41(7)	4.9	4.0	38.3	529	0.7	1.0
AlMCM-41	4.9	4.1	–	895	0.94	0.8
AlMCM-41	–	–	100	300	0.1	–

a_0, unit cell parameter; D_p, pore diameter; C_{REL}, relative crystallinity; S_{BET}, BET surface area; V_t, total pore volume; W_t, silica wall thickness ($W_t = a_0 - D_p$).

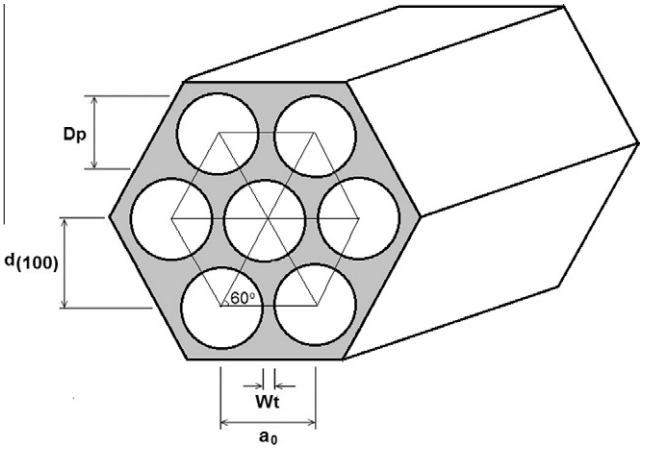

Fig. 3. Hexagonal arrangement of the mesoporous structure of the MCM-41 and hybrid materials, showing the mesoporous parameter (a_0), wall thickness (W_t), interplanar distance ($d_{(100)}$), and pore size diameter (D_p).

$$a_0 = \frac{2d_{(100)}}{\sqrt{3}} \quad (2)$$

$$W_t = a_0 - D_p \quad (3)$$

3.2. Dual templating mechanism

The dual template mechanism can be represented in Fig. 4, where both TPA^+ (tetrapropylammonium) and $CTMA^+$ (cetiltrimethylammonium) ions act as templates for the microporous ZSM-5 and mesoporous MCM-41 structures, respectively. The formation of the hybrid ZSM-5/MCM-41 is based on the charge compensation caused by the TPA^+ ions located on the surface of the mesoporous of the MCM-41.

The methodology of synthesis consisted firstly of the preparation of a reactive hydrogel of the ZSM-5, aged for 40 h at room temperature, and then crystallized at 90 °C, for generation of the zeolite seeds. The mesostructure was obtained by the addition of the surfactant CTMABr and water for these seeds, obtaining new micelles (see Fig. 4). The mixture was transferred for the autoclave and heated at 125 °C, from 6 to 12 days. In the seventh day of synthesis, was obtained the best order for the hybrid ZSM-5/MCM-41 material. Thus, the hybrid material selected for the catalytic pyrolysis of VGO was the HZSM-5/AlMCM-41(7). For 8 and 9 days of synthesis, poor ordered of mesoporous with crystalline zeolite phase was observed, while for 12 days, a predominant phase of ZSM-5 zeolite was obtained. The crystallization of the zeolitic phase was well observed in the system. Two steps of combinations were suggested for the investigated system. Depending of the time, the crystallization mechanism of the zeolite influences the structure ordering of the mesoporous phase. The ZSM-5 embedded in the bulk of MCM-41 must be readily obtained in the seventh day of synthesis, which was limited to the first step of crystallization. With the increasing of the time synthesis, some crystals of ZSM-5 could be produced and then impregnated to the MCM-41 already

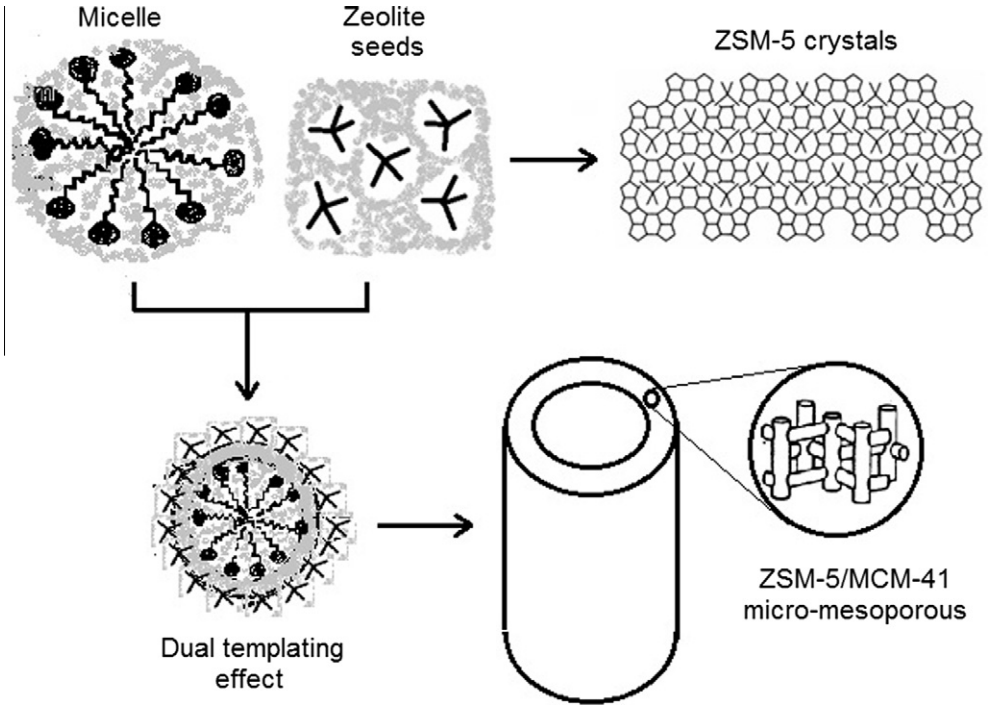

Fig. 4. Dual templating mechanism proposed for the synthesis of hybrid micro–mesoporous ZSM-5/MCM-41 materials.

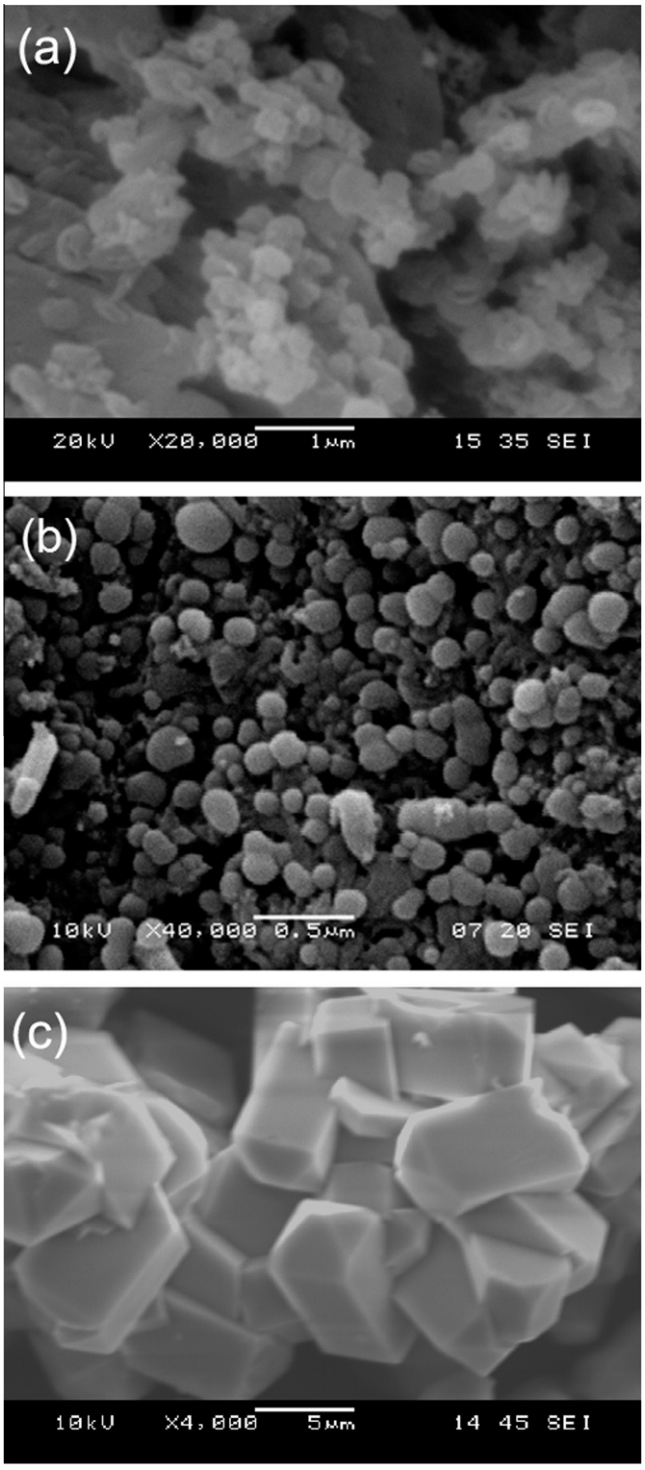

Fig. 5. SEM images for samples (a) hybrid ZSM-5/MCM-41 (×20,000); (b) AlMCM-41 (×40,000) and (c) ZSM-5 zeolite (×4000).

formed. In this way, the combination of the ZSM-5 with MCM-41 in the hybrid system could be obtained by the interconnection of the microporous of the ZSM-5 zeolite on the walls of the cylinder of the mesoporous of the MCM-41, as proposed in Fig. 4.

The hybrid material ZSM-5/MCM-41(7), with its microporous structure of the ZSM-5 zeolite, as confirmed by XRD, presented a negligible volume of micropores, indicating that the access of N_2 to the micropores was prevented. This factor might be an indication for the formation of the ZSM-5 structure in the core of the

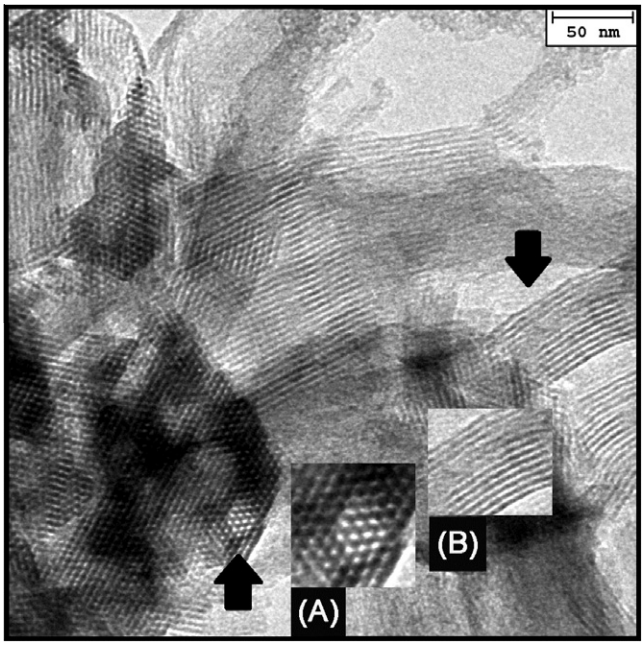

Fig. 6. TEM images for hybrid ZSM-5/MCM-41, showing the hexagonal arrangement of the mesoporous (A), and the longitudinal system of the mesopores (B).

Table 2
Medium, strong and total acidity of the H-MCM-41/ZSM-5(7), H-Al-MCM-41 and H-ZSM-5 samples determined by *n*-butylamine thermodesorption.

Sample	Acidity (mmol g^{-1})*		
	Medium	Strong	Total
HZSM-5/AlMCM-41(7)	1.28	0.75	2.03
AlMCM-41	0.89	0.10	0.99
HZSM-5	0.35	1.17	1.52

* Temperature ranges: medium (T = 100–300 °C); strong (T = 300–550 °C).

mesoporous MCM-41 particles. In this case, amorphous silica could be precipitated on the formed ZSM-5 crystallites, which prevented the access of nitrogen molecules to their micropores. That amorphous silica, which was generated during the formation of mesoporous ZSM-5 was already observed by Frunz et al. [30].

3.3. SEM and TEM analysis

Fig. 5(a) and (b) shows the Scanning Electron Micrographs (SEM) of the hybrid MCM-41/ZSM-5(7) and the ZSM-5 zeolite, respectively.

For an optimized structure of the hybrid, the MCM-41/ZSM-5(7) sample (Fig. 5(a)), plate-like particles with a hexagonal crystal habit and lengths up to 300 nm, were obtained. This morphology is commonly reported for aluminosilicates MCM-41 [31]. The presence of other phases or segregated particles, for instance, isolates crystals of ZSM-5 (Fig. 5(b)), which would indicate the formation of ZSM-5 independent of the mesoporous structure [32] were not observed, indicating the formation of a single type of solid, evidencing thus the formation of the hybrid structure.

Fig. 6 shows the Transmission Electron Micrography (TEM) of the hybrid ZSM-5/MCM-41. As can be observed, the hybridization of the zeolitic crystalline phase did not alter the ordering of the hexagonal and longitudinal arrangements of the mesoporous, even without the presence of the X-ray diffraction peaks relative to (210) and (300) Miller Index.

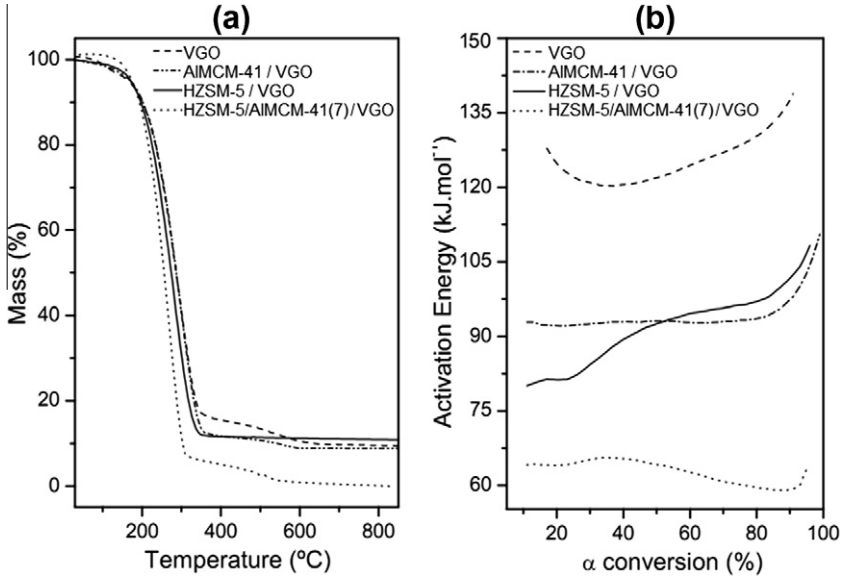

Fig. 7. TG/DTG curves for the samples: (a) only VGO mixed with 10% of catalyst and (b) activation energy curves in function of degree of conversion for thermal and catalytic pyrolysis of VGO.

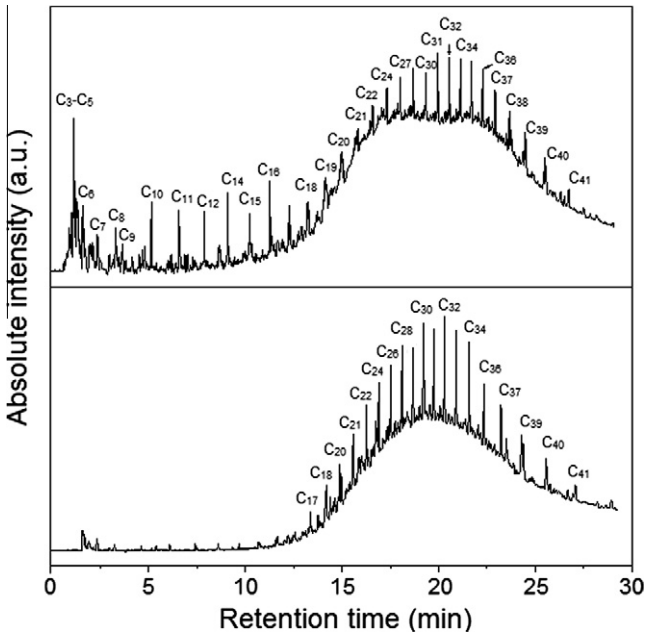

Fig. 8. Distribution of the hydrocarbon products in the carbon range, obtained by coupled pyrolysis-GC/MS: (a) pyrolysis of VGO and (b) pyrolysis of VGO mixed with 10% of hybrid HZSM-5/AlMCM-41 catalyst.

3.4. Acidity

In order to determine the density of acid sites for the HZSM-5/AlMCM-41(7), HAlMCM-41 and HZSM-5 samples, *n*-butylamine adsorption and thermodesorption by TG techniques were used. The acidity was measured considering that each *mol* of *n*-butylamine adsorbs on 1 mol of acid sites. The thermogravimetric results showed the profile of decomposition of the *n*-butylamine from the acid sites of the materials. The first temperature range, observed from 30 to 100 °C was attributed to physisorption and the loss of *n*-butylamine adsorbed onto the weak acid sites, while the second and third steps, considered in the ranges of 100–300 °C and 300–550 °C, were attributed to *n*-butylamine chemisorbed onto medium and strong acid sites, respectively. Furthermore it was possible to calculate, through the mass loss, the density of acid sites, as presented in Table 2. The experimental details and procedure for calculations were previously reported [22–26].

3.5. Catalytic conversion of VGO

The performance of the hybrid materials as catalyst for decomposition of the VGO was firstly determined by thermogravimetry. The profiles of the thermal behavior of the VGO alone and in presence of the samples of HZSM-5/AlMCM-41(7), HAlMCM-41 and HZSM-5 are shown in Fig. 7(a). In Fig. 7(b) is shown the activation energy as a function of the degree of conversion. The data related to the mass losses obtained from the thermogravimetry curves must be converted in data conversions before be submitted to kinetic treatment by the Vyazovkin model-free kinetic method. Assuming that the total mass loss corresponds to 100% of conversion, thus the mass losses in lower temperatures were normalized in relation to total mass loss originated the curve of conversion. The chromatograms of the products obtained from pyrolysis-GC/MS are shown in Fig. 8.

The pattern of thermal and catalytic degradation of heavy oils depends on several factors, being the main ones: the temperature and the type and the amount of catalyst added to the system. The reaction rate and others kinetic parameters for each system should be determined through experimental data, however due to complexity of the hydrocarbons degradation reactions, the conventional methods of determination of the kinetic data are difficult of be applied. Therefore, in this study was applied non-isothermal model-free kinetic of Vyazovkin [33] to determine the activation energy for the reaction of VGO degradation in the presence of catalysts without the need of a model of reaction rate in function of the reactants concentrations. Eq. (4) represents the integrated form of the model-free kinetic proposed by Vyazovkin.

$$\ln\left(\frac{\beta}{T_\alpha^2}\right) = \ln\left[\frac{R \cdot k_0}{E_a \cdot g(\alpha)}\right] - \frac{E_a}{R} \cdot \frac{1}{T_\alpha} \tag{4}$$

where α is the conversion of the VGO degradation reaction; T_α is the temperature to reach the conversion α; β is the heating rate; R is universal gas constant; k_0 is Arrhenius pre-exponential factor; E_a

is the activation energy for a certain conversion α and $g(\alpha)$ is the integral of the kinetic model of reaction rate in function of the conversion. In most of the cases the function $g(\alpha)$ does not present a defined form and after the model fitting, $g(\alpha)$ become implicit in the linear coefficient obtained. Eq. (4), indicates that a plotting of $ln(\beta/T_\alpha^2)$ versus $1/T_\alpha$ gives a straight line and from its slope can be determined the activation energy.

The Vyazovkin's model-free kinetic algorithms were applied to calculate the activation energy (E_a) for the pyrolysis process of VGO pure and in the presence of the catalysts (Fig. 7(b)). The E_a was *ca.* 60 kJ mol^{-1} for the hybrid catalyst HZSM-5/AlMCM-41(7); *ca.* 80–90 kJ mol^{-1} for the mesoporous molecular sieve H-AlMCM-41 as well for the zeolite HZSM-5, and ca. 130 kJ mol^{-1} for thermal degradation of VGO alone. It could be concluded that the hybrid catalyst led to lower activation energy, and presented a significant potential for the catalytic processing of VGO degradation due to the combination of acidic sites in the microporous of the HZSM-5 combined with the accessibility of this sites through the mesoporous of AlMCM-41 structure, resulting in a higher efficiency of the hybrid material. It was observed that E_a values decrease with the increase of the acid properties of catalyst. These results suggest that the catalyst acidity is one of the most important parameters in the reaction for catalytic pyrolysis of this VGO residue.

In Fig. 8, analyzing the chromatograms of the products of the VGO pyrolysis with and without catalyst, it can be shown that VGO alone suffers thermal degradation for hydrocarbons in the carbon range from C_{17} to C_{41}, with high activation energy. However, when the hybrid material was added to VGO, light fraction could be obtained, typically in the range of C_3–C_5 (liquefied petroleum gas); and middle distillates, C_6–C_{10} (gasoline) and C_{11}–C_{16} (diesel), with low activation energy, proving the catalytic effect of the hybrid material for the pyrolysis of VGO residue. The LPG and gasoline fractions were produced due to strong acid sites combined with the microporosity of the HZSM-5 zeolite, whereas the diesel fraction was attributed to the mesoporosity associated to mild acid sites of the AlMCM-41.

4. Conclusions

The hybrid material that was developed in two-step crystallization process using dual templates, combined the high catalytic activity of the zeolites with the larger pore size of the molecular sieves. In the sample ZSM-5/AlMCM-41(7), the formation of the hybrid led to the growth of zeolitic crystallites of ZSM-5 embedded into the bulk of the mesoporous AlMCM-41 material, furthermore leading to a stronger surface acidity in relation to mild acid sites of the AlMCM-41 molecular sieve. The physicochemical characterizations of the materials by SEM and N_2 adsorption–desorption showed the morphological compatibility and a high surface area of the synthesized hybrid material when compared with the literature data. The hydrothermal treatment results in the formation of a ordered MCM-41 mesoporous material with a crystalline wall of the microporous ZSM-5 zeolite. The use of hybrid catalyst decreased the activation energy, which favors the catalytic reaction for the pyrolysis of vacuum gasoil. This is probably due to the combination of strong acidic sites and stability of the HZSM-5 zeolite with the better accessibility of acidic sites through the large pores of the MCM-41 structure, resulting in a highly efficient catalyst. The obtained products from pyrolysis of VGO in the presence of the hybrid catalyst were typically in the range of C_3–C_5 (liquefied petroleum gas) and middle distillates, mainly C_6–C_{10} (gasoline range) and C_{11}–C_{16} (diesel). The pyrolysis of VGO without catalyst produced mainly hydrocarbons in the range of C_{17}–C_{43}.

Acknowledgments

This work was supported by the National Council of Technological and Scientific Development (CNPq, Brazil). One of us (A.C.F.C.) acknowledges the Post-Graduation Program in Chemistry at the Federal University of Rio Grande do Norte, for the Post-Doctoral fellow and research funding.

References

[1] M. Reichingera, W. Schmidtb, V.V. Narkhedea, W. Zhangc, H. Giesa, W. Grünertd, Microporous Mesoporous Mater. 164 (2012) 21.
[2] V. Antochshuk, A.S. Araujo, M. Jaroniec, J. Phys. Chem. B 104 (2000) 9713.
[3] M.J.B. Souza, B.A. Marinkovic, P.M. Jardim, A.S. Araujo, A.M.G. Pedrosa, R.R. Souza, Appl. Catal., A Gen. 316 (2007) 212.
[4] A.S. Araujo, S.A. Quintella, A.C.S.L.S. Coutinho, Adsorption 15 (2009) 306.
[5] F.L. de Castro, J.G. Santos, G.J.T. Fernandes, A.S. Araujo, V.J. Fernandes, M.J. Politi, Microporous Mesoporous Mater. 102 (2007) 258.
[6] S. Ramirez, J.M. Dominguez, L.A. Garcia, M.A. Mantilla, C.A. Flores, J. Salmones, D. Jeronimo, Pet. Sci. Technol. 22 (2004) 119.
[7] R.A. Garcia, D.P. Serrano, D. Otero, J. Anal. Appl. Pyrolysis 74 (2005) 379.
[8] J.S. Beck, J.C. Vartuli, W.J. Roth, M.E. Leonowicz, C.T. Kresge, K. Schmitt, C.T.W. Chu, D.H. Olson, E.W. Sheppard, S.B. McCullen, J.B. Higgins, J. Am. Chem. Soc. 114 (1992) 10834.
[9] C.T. Kresge, M.E. Leonowicz, W.J. Roth, J.C. Vartuli, Nature 359 (1992) 710.
[10] L. Huang, W. Guo, P. Deng, Z. Xue, Q. Li, J. Phys. Chem. B 104 (2000) 2817.
[11] D. Trong On, D. Lutic, S. Kaliaguine, Microporous Mesoporous Mater. 44 (2001) 435.
[12] M.L. Gonçalves, L.D. Dimitrov, M.H. Jordão, M. Wallau, E.A. Urquieta-González, Catal. Today 133 (2008) 69.
[13] E.F.B. Silva, M.P. Ribeiro, A.C.F. Coriolano, A.C.R. Melo, A.G.D. Santos, V.J. Fernandes, A.S. Araujo, J. Therm. Anal. Calorim. 106 (2011) 793.
[14] E.F.B. Silva, M.P. Ribeiro, L.P.F.C. Galvao, V.J. Fernandes, A.S. Araujo, J. Therm. Anal. Calorim. 103 (2011) 465.
[15] J.G.A. Pacheco, E.C. Graciliano, A.O.S. Silva, M.J.B. Souza, A.S. Araujo, Catal. Today 107 (2005) 507.
[16] A.S. Araujo, V.J. Fernandes, G.J.T. Fernandes, Thermochim. Acta 392 (2002) 55.
[17] S.A. Araujo, A.S. Araujo, N.S. Fernandes, V.J. Fernandes, M. Ionashiro, J. Therm. Anal. Calorim. 99 (2010) 465.
[18] A. Marcilla, M.R. Hernandez, A.N. Garcia, Appl. Catal., A Gen. 341 (2008) 181.
[19] M.J.B. Souza, A.S. Araujo, A.M.G. Pedrosa, B.A. Marinkovic, P.M. Jardim, E. Morgado Jr, Mater. Lett. 60 (2006) 2682.
[20] S. Brunauer, P.H. Emmett, E. Teller, J. Am. Chem. Soc. 60 (1938) 309.
[21] E.P. Barrett, L.G. Joyner, P.P. Halenda, J. Am. Chem. Soc. 73 (1951) 373.
[22] A.O.S. Silva, M.J.B. Souza, A.S. Araujo, Int. J. Inorg. Mater. 3 (2001) 461.
[23] M.J.B. Souza, A.O.S. Silva, V.J. Fernandes, A.S. Araujo, J. Therm. Anal. Calorim. 79 (2005) 425.
[24] A.S. Araujo, V.J. Fernandes, S.A. Verissimo, J. Therm. Anal. Calorim. 59 (2000) 649.
[25] A.S. Araujo, V.J. Fernandes, I. Giolito, L.B. Zinner, Thermochim. Acta 223 (1993) 129.
[26] V.J. Fernandes, A.S. Araujo, G.J.T. Fernandes, J. Therm. Anal. Calorim. 56 (1999) 275.
[27] S. Vyazovkin, V. Goryachko, Thermochim. Acta 194 (1992) 221.
[28] B. Saha, A.K. Maiti, A.K. Ghoshal, Thermochim. Acta 444 (2006) 46.
[29] K.S.W. Sing, D.H. Everett, R.A.W. Haul, L. Moscou, R.A. Pierotti, J. Rouquerol, T. Siemieniewska, Pure Appl. Chem. 57 (1985) 603.
[30] L. Frunz, R. Prins, G.D. Pirngruber, Microporous Mesoporous Mater. 88 (2006) 152.
[31] S. Liu, L. Kong, X. Yan, Q. Li, A. He, Stud. Surf. Sci. Catal. 156 (2005) 379.
[32] A.A. Campos, L. Dimitrov, C.R. Silva, M. Wallau, E.A. Urquieta-Gonzalez, Microporous Mesoporous Mater. 95 (2006) 92.
[33] S. Vyazovkin, C.A. Wight, Int. Rev. Phys. Chem. 17 (1998) 407.